Catalyst Deactivation During Rhodium Complex-Catalyzed Propargylic C–H Activation

Saskia Möller,[a] Nora Jannsen,[a] Julia Rüger,[a] Hans-Joachim Drexler,[a] Moritz Horstmann,[a] Felix Bauer,[b] Bernhard Breit,*[b] and Detlef Heller*[a]

This paper is dedicated to Professor Barry Trost for the outstanding importance of his work in the field of homogeneous catalysis.

Abstract: Detailed mechanistic investigations on our previously reported synthesis of branched allylic esters by the rhodium complex-catalyzed propargylic C–H activation have been carried out. Based on initial mechanistic studies, we present herein more detailed investigations of the reaction mechanism. For this, various analytical (NMR, X-ray crystal structure analysis, Raman) and kinetic methods were used to characterize the formation of intermediates under the reaction conditions. The knowledge obtained by this was used to further optimize the previous conditions and generate a more active catalytic system.

Introduction

The synthesis of allylic products from easily available starting materials is an important research topic in modern organic synthesis.[1] The allylic moiety enables further functionalizations such as cyclopropanation, epoxidation or hydroboration, among others.[1a] Besides, the generation of prochiral branched allylic products is a valuable tool in asymmetric synthesis.[1a] Significant progress in this research field was achieved by transition metal catalysis, especially by allylic substitution[2] and allylic C–H oxidation.[3] However, these methods have intrinsic disadvantages, such as the presence of a leaving group in the substrate or the use of stoichiometric amounts of oxidant. For the synthesis of linear allylic products some more atom economic methods mostly based on palladium catalysis were first published by Trost and Yamamoto.[4] In a seminal work, Breit et al. reported the first example of the branched selective synthesis of allylic esters by addition of carboxylic acids to terminal alkynes applying rhodium catalysis (Scheme 1).[5] This rhodium complex catalyzed propargylic C–H activation is

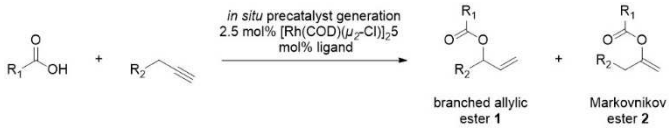

Scheme 1. Rhodium complex-catalyzed formation of allylic esters.

superior to competing methods due to its intrinsic redox neutrality and atom economy.[5] This reaction is characterized by high yields and excellent regio- (up to >98:2 branched to Markovnikov ester) and enantio- (up to 93% *ee*) selectivities.[5,6] Beyond carboxylic acids,[5,6,7] the potential of this reaction could also be applied to sulfonylhydrazines, pyrazoles and ketones.[8] Apart from this, the variation of the alkyne enables a considerable increase in the range of products.[9] First evidences of the complexity of this reaction were published by the groups of Breit and Heller.[5,6,7,10]

Preliminary directional studies on the reaction kinetics of this rhodium complex catalyzed propargylic C–H activation were performed by in situ IR spectroscopy.[10a] Using the initial rate method, the reaction was found to show zero-order dependence in substrates and first-order behavior in catalyst. Both product formation and substrate consumption can therefore be expected to be constant over time. However, this does not correspond to the in situ IR measurements, since a decrease in reaction rate was detected with increasing conversion.[10a] These obvious contradictions could not be explained so far and are part of more detailed mechanistic and kinetic investigations in the context of the present work. In addition to extensive NMR studies on isolated elementary steps of the published catalytic cycle,[10a] isolable intermediates were characterized by X-ray crystal structure analysis. The combination of these findings provides the basis for further optimizations of the catalytic propargylic C–H activation and should allow to extend applications of this reaction.

[a] Dr. S. Möller, N. Jannsen, Dr. J. Rüger, Dr. H.-J. Drexler, M. Horstmann, Prof. Dr. D. Heller
Leibniz-Institut für Katalyse e.V.
Albert-Einstein-Str. 29a, 18059 Rostock (Germany)
E-mail: detlef.heller@catalysis.de

[b] Dr. F. Bauer, Prof. Dr. B. Breit
Institut für Organische Chemie
Albert-Ludwigs-Universität Freiburg
Albertstr. 21, 79104 Freiburg (Germany)
E-mail: bernhard.breit@chemie.uni-freiburg.de

Supporting information for this article is available on the WWW under https://doi.org/10.1002/chem.202102219

Results and Discussion

In the context of the present work, in situ operando NMR investigations of rhodium complex catalyzed propargylic C–H activation were performed for the first time. When monitoring the reaction of benzoic acid and 1-octyne as model compounds at T = 70 °C using the in situ system $[Rh(COD)(\mu_2\text{-}Cl)]_2$/DPEPhos as the catalyst by multinuclear NMR spectroscopy for t = 870 min (14.5 h) complex ^{1}H NMR spectra are obtained (Figure S1). It is remarkable that in addition to the esters described so far (branched allylic ester **1** and Markovnikov ester **2**), another product is obviously formed, which most likely possesses vinylic C–H atoms according to its NMR signals (ddq, δ = 4.94 ppm; ddq, δ = 5.07 ppm). It is known from the literature that rhodium and other transition metal complexes catalyze the isomerization of alkynes[11] and allenes[12] into the corresponding dienes. A reference measurement confirms the hypothesis that the light gray marked signals in the range of 5.11–4.91 ppm are caused by 1,3-octadiene **3**, which is generated due to alkyne or allene isomerization during the catalytic cycle[13] (for NMR data see Supporting Information Figure S2). In a test experiment using 1,3-octadiene as substrate under similar conditions (2.5 mol% catalyst, 70 °C, 16 h see Supporting Information Figure S3) no conversion was detected. Due to this we assume the generation of **3** by isomerization to be irreversible.

A plot of the corresponding concentrations of the substrates and products as a function of time gives the concentration-time diagram shown in Figure 1. The generated 1,3-octadiene **3** is formed in approximately the same concentration as the Markovnikov ester **2**.

Evidently, no linear dependency for substrate decrease or product increase can be observed, as it would be expected from the previous kinetic investigations (zero order dependence) using in situ IR measurements.[10a] However, if the concentration of the active catalyst decreases during the reaction, for example due to the formation of a catalytically inactive rhodium complex, the decrease in the rate of product formation in the reaction progress, as shown in Figure 1, can be easily explained. As the formation of the corresponding catalyst species was also followed by ^{31}P NMR spectroscopy, the evaluation of these data should provide an explanation (Figure S4). Despite the large number of signals, clear trends can be observed. For example, during the reaction a broad doublet of an unknown species disappears at 16.2 ppm and another doublet at 26.3 ppm grows in intensity. The signals of the σ-allyl complex (**4** in blue), which corresponds to the "resting state"[14] complex as active catalyst,[10a] can be clearly assigned. When crystals of the σ-allyl complex are dissolved in 1,2-dichloroethane (Figure S5), signals of another species appear in the ^{31}P NMR spectrum (dd, δ = 34.9 ppm; dd, δ = 30.6 ppm). These can be assigned to a π-allyl complex (**5** in yellow) in equilibrium with the σ-allyl complex **4**.[10a] The ^{31}P NMR spectra confirm that no phosphorus-containing rhodium complex remains constant over the reaction time, which supports the above-made assumption of a non-constant catalyst concentration (Figure 2). Furthermore, a very prominent set of signals (Figure S4, marked in red, dd, δ = 35.6 ppm; dd, δ = 32.8 ppm) is present almost quantitatively at the end of the reaction. If the integrals of the individual signal sets are related to each other, time-dependent data proportional to the concentration of the rhodium species can be visualized.

At the beginning of the reaction approx. 60 % of the σ-allyl complex **4** ("resting state" complex, blue) and 20 % of the π-allyl complex **5** (active catalyst, yellow) are present. The time dependence of the complex **6** (marked red), which is present almost quantitatively at the end of the reaction, possibly indicates the formation of a catalytically inactive species.

Numerical rank matrix analyses are often used to determine the number of linearly independent partial reactions. However, this problem can also be solved graphically, using so-called *concentration diagrams*.[15] This not only determines the number of linearly independent partial reactions, but also provides information about the stoichiometric coefficients of the reaction.[15] The plot shown in Figure 3 shows an approximately linear relationship between the concentrations of the products (Markovnikov ester **2** plotted against the branched allylic ester **1**). This indicates that **2** is not formed from **1** (or vice versa) but

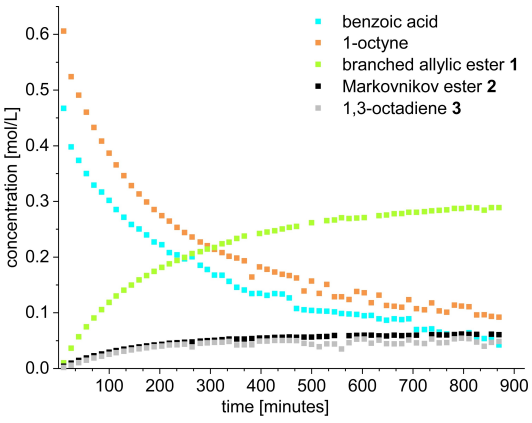

Figure 1. Concentrations of substrates and products obtained from ^{1}H NMR spectra (Figure S1) as a function of time.

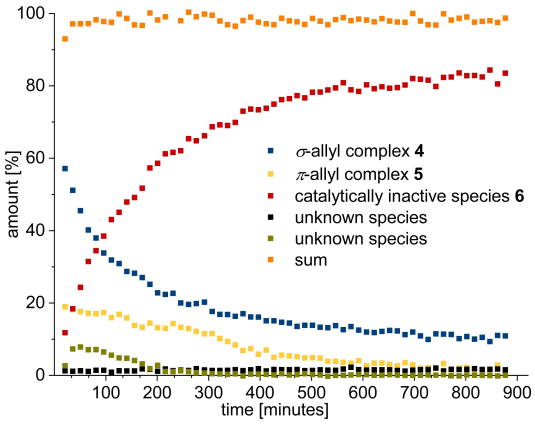

Figure 2. Ratio of rhodium complexes obtained from ^{31}P NMR spectra (Figure S4) as a function of time; the sum of all signals remains constant over the course of the reaction within the limits of measurement accuracy.

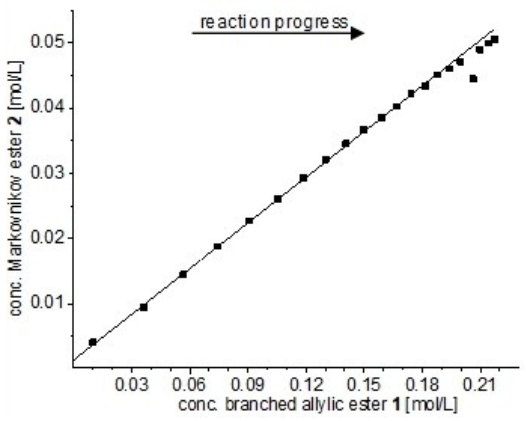

Figure 3. Concentration diagram according to Mauser;[15] plot of the concentration of the Markovnikov ester **2** as a function of the concentration of the branched allylic ester **1** determined from ^{1}H NMR data (Figure S1).

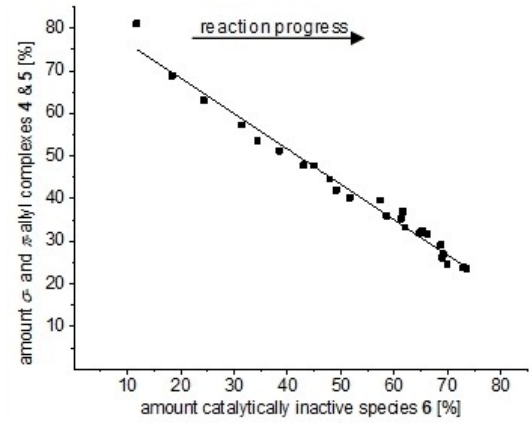

Figure 4. Concentration diagram according to Mauser;[15] plot of the percentage of active catalyst species (σ- and π-allyl complex, **4** and **5**) as a function of the percentage of catalytically inactive species **6** determined from the ^{31}P NMR data (Figure S4).[16]

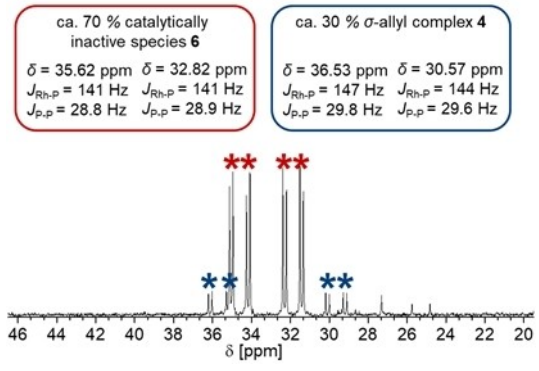

Figure 5. ^{31}P NMR spectra of the catalyzed addition of [benzoic acid] = 0.47 mol/L and [1-octyne] = 0.61 mol/L using the in situ generated precatalyst [[Rh(DPEPhos)(μ_2-Cl)]$_2$] **7** = 0.023 mol/L in 1,2-dichloroethane-d_4 at 70 °C after 900 minutes; σ-allyl complex (**4**, *); unknown species which may be catalytically inactive (**6**, *).

that both products are the result of a parallel reaction, which is in line with the mechanistic proposal made earlier.[10a]

In contrast to the analysis of the concentration data for the products, the plot of the percentage of active catalyst species (**4** and **5**) as a function of the probably inactive species **6** gives a straight line which shows that the species primarily present at the end of the reaction is formed from the mixture of σ- and π-allyl complex in the sense of a subsequent reaction (Figure 4).

The ^{31}P NMR spectrum of the addition of benzoic acid to 1-octyne catalyzed by [Rh(COD)(μ_2-Cl)]$_2$/DPEPhos (in situ) at 70 °C in 1,2-dichloroethane almost exclusively contains two signal sets after 15 h of reaction time (Figure 5). Precipitation of rhodium complexes from this reaction mixture is described in the synthetic procedures (Supporting Information). By manual sorting under inert atmosphere, the separation of crystals suitable for X-ray crystal structure analysis was possible (Figure S6).

The connectivity found in the molecular structure (Figure 6) is in favor of the assumed formation of the already discussed σ-allyl complex **4**[10a] (Figure S7, right). It shows the rhodium(III) center in octahedral coordination geometry surrounded by the diphosphine, chloride, a benzoate ligand and a vinyl ligand that originates from 1-octyne. However, bond lengths of the alkyl chain point to a different position of the C–C double bond (Figure S7) and indicate the presence of the σ-vinyl complex with a terminal double bond instead of the σ-allyl species. Further details on the characterization of this compound by multinuclear NMR experiments can be found in the Supporting Information (Figures S7–S14).

To further distinguish between the σ-vinyl and σ-allyl complex, Raman measurements were carried out (Figure 7) allowing for an unequivocal assignment of the position of carbon-carbon multiple bonds. The Raman bands were assigned by quantum mechanical spectra simulations (Supporting Information) and reference measurements of the DPEPhos ligand and the benzoic acid (Figure S15 and S16). The characteristic stretching vibration of the C–C double bond in the σ-allyl complex **4** appears at 1655 cm^{-1} while in the σ-vinyl complex **6**

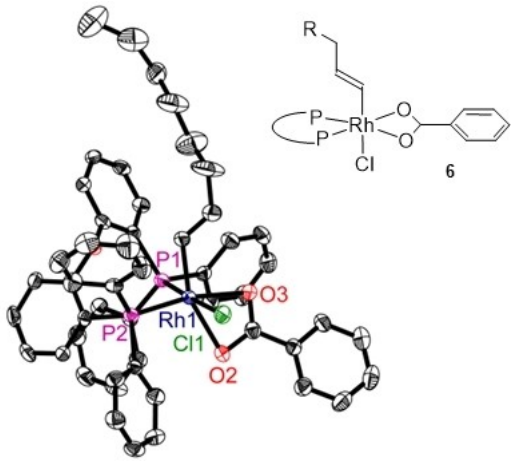

Figure 6. Molecular structure of the σ-vinyl complex **6**. Hydrogen atoms are omitted for clarity (ORTEP, 30% probability ellipsoids).

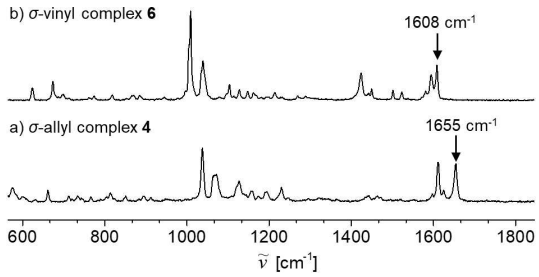

Figure 7. Raman spectra of a) the σ-allyl complex **4**, C=C stretching vibration at 1655 cm^{-1}; b) the σ-vinyl complex **6**, vinylic C=C stretching vibration at 1608 cm^{-1}.

it is found bathochromically shifted by 47 cm^{-1} (Figure 7). The band at 1608 cm^{-1} is therefore in the typical range for terminal carbon-carbon double bonds.[17]

The σ-vinyl complex **6** is obviously responsible for catalyst deactivation during the reaction, which becomes dominant with increasing conversion. An NMR scale experiment using **6** as catalyst proves that this species is indeed catalytically inactive (Figure S17).

To elucidate the mechanism for the formation of the catalytically inactive σ-vinyl complex **6**, the isolable σ-allyl complex **4** (i.e. the "resting state" compound) was reacted with all reactants at both room temperature as well as at $T = 70\,^{\circ}C$ and examined using ^{31}P NMR spectroscopy (Figure S18). These experiments clearly show that the catalytically inactive σ-vinyl complex **6** is formed from reaction of the σ-allyl compound **4** with 1-octyne at 70 °C. To further verify whether this reaction sequence corresponds to an exchange of the alkyl ligand, the σ-allyl complex **4** was reacted with trimethylsilylacetylene **8**. In fact, it was possible to isolate a $SiMe_3$ substituted σ-vinyl complex **9**, which proves the assumption of an exchange reaction and excludes for example a simple (thermal) rearrangement (Figure 8).

If the precatalyst $[Rh(DPEPhos)(Cl)]_2$ **7** is reacted with an excess of benzoic acid at 70 °C, the additional rhodium species **10** was formed (Scheme 2). **10** can be isolated and characterized by NMR spectroscopy. It corresponds to a product of the oxidative addition of benzoic acid to the monomerized precatalyst **11** and gives a hydride signal at −15.15 ppm (dt, $J_{Rh-H} = 11.8$ Hz, $J_{P-H} = 17.4$ Hz) in ^1H NMR spectrum. By ^1H-^{31}P-HMBC NMR spectroscopy (Figure S19) the hydride signal could be clearly assigned to the doublet in the ^{31}P NMR spectrum at 43.03 ppm (Figure 9).

If the precatalyst is generated in situ and reacted with benzoic acid, another benzoate complex **12** (27.86 ppm, d in ^{31}P NMR spectrum) is formed in addition to the hydrido benzoate complex (Figure S20), presumably by disproportionation of **10** (Scheme 2).

In this rhodium(III) species the hydride ligand is replaced by another chlorine atom, forming the dichlorido benzoate complex **12**. The molecule was characterized by NMR and X-ray crystal structure analysis (Figures S21) and possesses an octahedral rhodium(III) center coordinated with DPEPhos, a benzoate

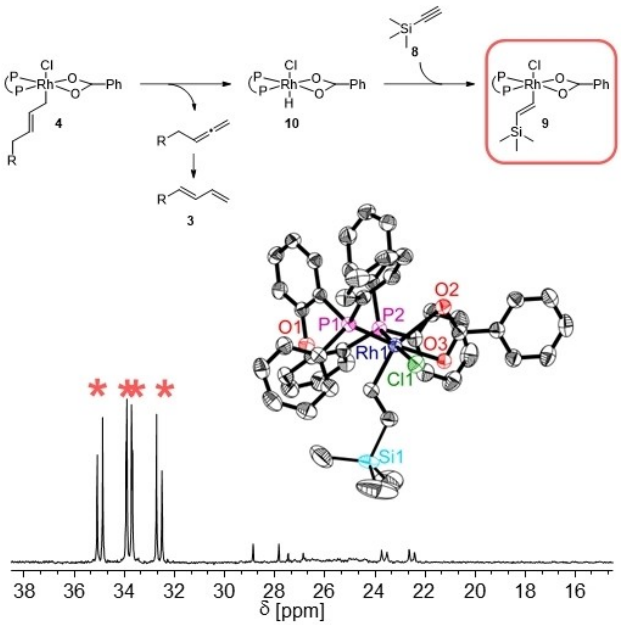

Figure 8. Synthesis of a $SiMe_3$ substituted σ-vinyl complex **9**, ^{31}P NMR spectrum of the reaction of σ-allyl complex **4** with an excess of trimethylsilylacetylene **8** in 1,2-dichloroethane-d_4 and the molecular structure of the $SiMe_3$ substituted σ-vinyl complex **9**. Hydrogen atoms are omitted for clarity (ORTEP, 30% probability ellipsoids).

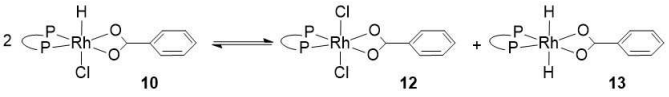

Scheme 2. Disproportionation of the monohydride benzoate complex **10**.

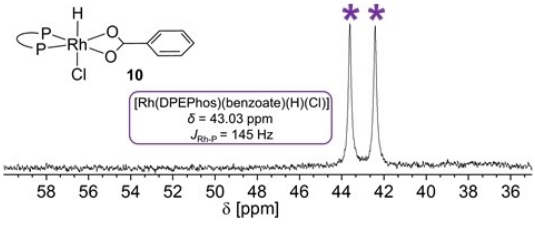

Figure 9. ^{31}P NMR spectrum of the conversion of $[Rh(DPEPhos)(\mu_2\text{-}Cl)]_2$ and benzoic acid (in the ratio 1:54) at 70 °C in 1,2-dichloroethane-d_4.

group and two chloride ligands. During the reaction it can be observed in ^1H NMR (Figure S22) that the free cyclooctadiene generated as a result of the in situ production of the precatalyst reacts to cyclooctene. If **10** is converted with 1-octyne, an immediate formation of the σ-allyl **4** and σ-vinyl complex **6** can already be observed at room temperature (Figure S23). The reaction is too fast for kinetic NMR investigations. However, if **12** is converted with 1-octyne, the reaction is slow enough for NMR spectroscopic monitoring. This NMR spectroscopic monitoring confirms the formation of the σ-vinyl species **6** from this benzoate complex **10** (Figure S24). Additional validation of this

conversion is provided by the concentration diagram of these data (Figure 10).

The reaction from **12** to **6** is likely to take place via benzoate complex **10**. The mechanism for this step is still unclear, but due to the excess of 1-octyne, a reaction of it seems to be a likely hydride source for the formation of **10**. If the reaction from **10** to **6** takes place immediately at room temperature, then it can be assumed that the formation of the monohydride species **10** from **12** is the slowest step of this catalytic reaction. The resulting linear relationship with a slope of approximately −45° proves that the catalytically inactive σ-vinyl complex **6** is formed pseudo directly from the benzoate complex **12** (Scheme 3).

In order to relate this deactivation path to the original catalysis, initial rates of these individual steps as well as of the rhodium complex catalyzed propargylic C–H activation, i.e. the total reaction, were determined (Table 1).[18]

This analysis shows that formation of the benzoate complex **12** and the σ-vinyl species **6** occur at approximately equal rates. The benzoate complex **12** is formed with a rate of $2.9 \cdot 10^{-6}$ mmol/mL·s but it is also converted into the catalytically inactive σ-vinyl species **6** in the presence of 1-octyne ($2.5 \cdot 10^{-6}$ mmol/mL·s). Its stationary concentration during catalysis is thus very small. With these initial rates it can now be explained why only a small portion of **12** (approx. 4%) could be detected during monitoring of the catalytic reaction (Figure S3, grey-blue species). Although the formation of the σ-vinyl complex **6** is by an order of magnitude slower than the actual catalytic reaction (Table 1), the formation of the catalytically inactive species occurs *irreversibly*. Thus, it can be concluded that almost all rhodium catalyst is irretrievably deactivated during propargylic C–H activation under the used standard reaction conditions. Even repeated addition of substrate would not lead to further product formation.

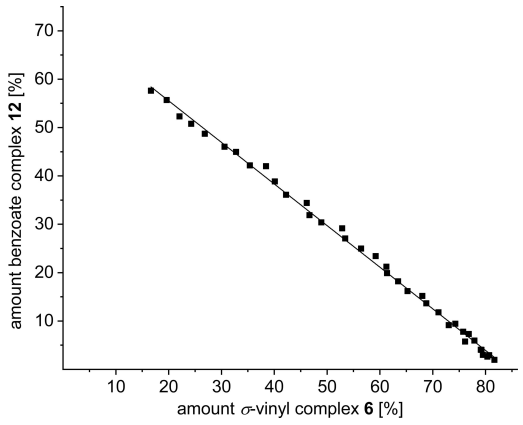

Figure 10. Concentration diagram according to Mauser;[15a] plot of the percentage of the benzoate complex **12** determined from ^{31}P NMR data as a function of the percentage of the σ-vinyl complex **6**.

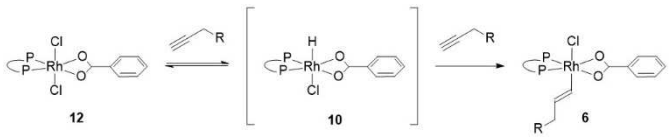

Scheme 3. Reaction of the dichloride benzoate complex **12**, forming the σ-vinyl complex **6**.

Table 1. Initial rates of the total reaction as well as the formation of the benzoate complex 12 and the σ-vinyl species **6**. ([catalyst] = 0.0023 mol/L, [alkyne] = 0.61 mol/L, [benzoic acid] = 0.47 mol/L in 1,2-dichloroethane-d_4 at 70 °C)

reaction sequence	Initial rates [mmol/mL·s]
total reaction (product formation)	$4.1 \cdot 10^{-5}$
formation benzoate complex **12**	$2.9 \cdot 10^{-6}$
formation σ-vinyl complex **6**	$2.5 \cdot 10^{-6}$

The presented results significantly extend the initially proposed reaction pathway[10a] (Figure S25) and allow for the refinement of the mechanistic picture (Figure 11). After an experimentally confirmed monomerization of **7** to **11** of the precatalyst **7**,[19] coordination of 1-octyne occurs, as described earlier.[10a] However, the results also indicate that the alkyne complex **14** is not asymmetric, as previously assumed but has a symmetrical structure and is neutral in nature due to the coordination of two alkyne molecules.[20] Based on NMR data (d, $\delta = 23.3$ ppm, $J_{RhP} = 117$ Hz) and comparison with literature data ([RhCl(NBD)(DPEPhos)], d, $\delta = 15.5$ ppm, $J_{RhP} = 120$ Hz),[21] this compound is most likely a rhodium(I) complex that possesses a fivefold coordinated metal center (Figure S26). Furthermore, its formation is reversible.[22] Subsequent ligand exchange with benzoic acid and intramolecular alkyne protonation leads via transition state **15** to the vinyl species **16**. Competing dimerization of the alkyne from complex **14** is also formally feasible but could be excluded experimentally.[23] From **16** reductive elimination explains the formation of the side product, the Markovnikov ester **2** (Figure S27). β-Hydride elimination leads via the allene hydrido complex **17** to σ-/π-allyl equilibrium **4** and **5**.[10a] Reversible reductive elimination of the branched allyl ester **1** from π-allyl complex **5** closes the catalytic cycle and regenerates **11**.[10a]

The formation of the side product 1,3-octadiene **3** could likely be explained by the hydrometallation of the internal double bond of the allene ligand in complex **17**. The so formed internal σ-allyl complex **18** could react by a consecutive reductive elimination to the monohydride benzoate complex **10** and release **3**.

Although a reaction of the precatalyst **7** [Rh(DPEPhos)(μ_2-Cl)]$_2$ with benzoic acid at room temperature was excluded in our earlier work,[10a] new investigations at 70 °C, i.e. under standard reaction conditions, have shown that a parallel reaction in fact takes place. The benzoate complex **10** from this conversion and its formation was explored in detail. Thus, in the presence of an olefin or diolefin (like COD due to in situ precatalyst generation) the benzoate complex **12** is visible, as a result of a disproportionation of **10** and hydrogenation of the respective olefin by **13**. The catalyst deactivation associated with benzoate complexes **10** (or **12**) is an important key step. By coordinating 1-octyne as a vinyl ligand to the benzoate

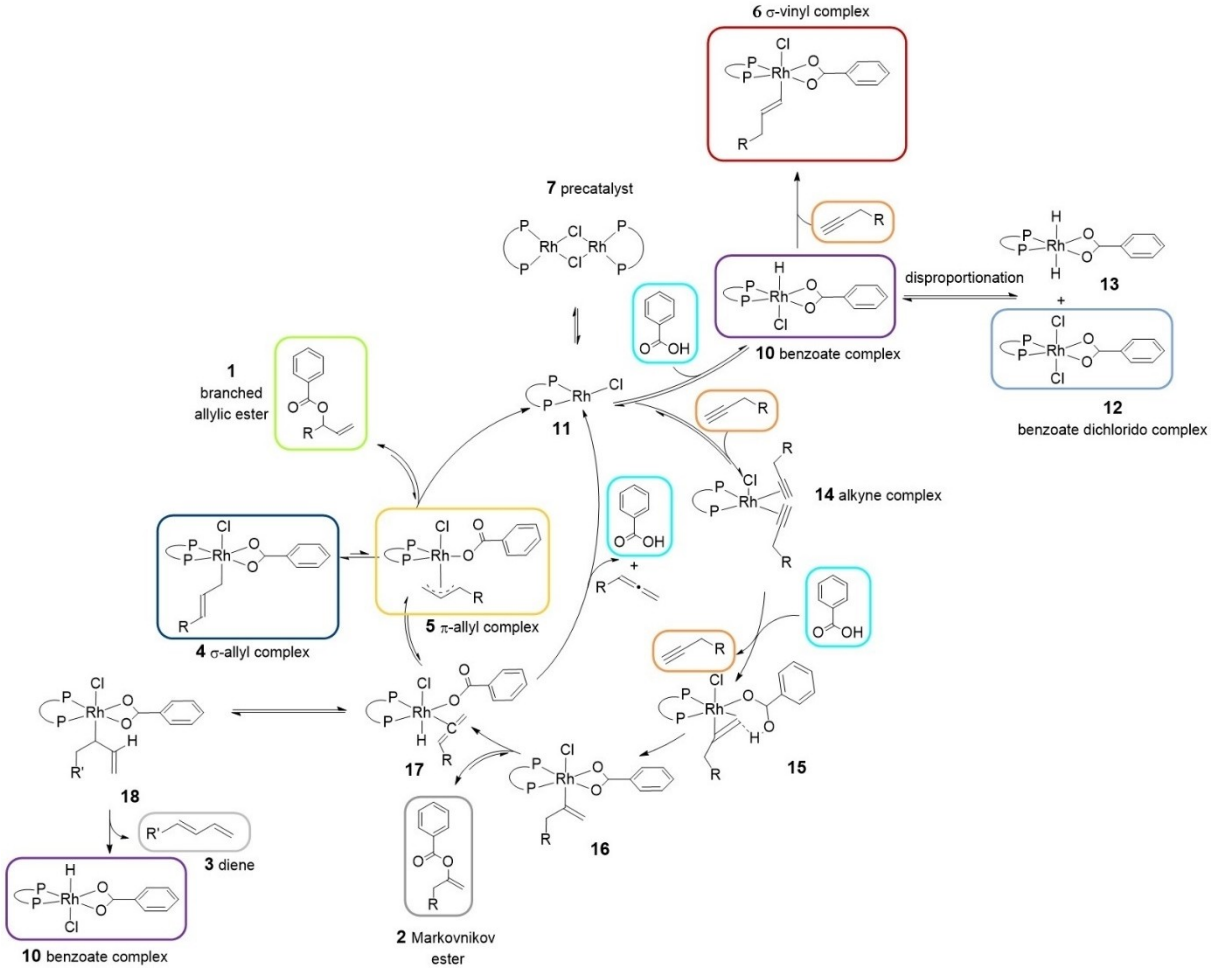

Figure 11. Modified reaction mechanism of rhodium complex catalyzed propargylic C–H activation based on the results presented in this work.

complex **10**, the catalytically inactive σ-vinyl complex **6** is formed irreversibly.

In order to minimize the formation of the σ-vinyl complex **6**, now recognized as the reason for catalyst deactivation, the formation of its precursor, the benzoate complex **10** must therefore be reduced as much as possible. Due to this, it is desirable to increase the concentration of alkyne in solution at constant benzoic acid concentration to facilitate the alkyne coordination to **11** to form **14**. By this, the actual catalytic cycle is preferred over the competitive formation of the benzoate complex **10** and the resulting catalytically inactive σ-vinyl species **6**. In fact, it could be shown experimentally that an increase of concentration of alkyne from 1.2 eq. to 4.7 eq. in the rhodium complex catalyzed addition of benzoic acid to 1-octyne leads to a reduced formation of the catalytically inactive σ-vinyl compound **6** (Figure S28).[24] The results show that a significantly lower catalyst/substrate ratio is possible and the catalyst concentration can be reduced from initially 5 mol% to 2.5 mol% with unchanged high selectivity (Scheme 4).

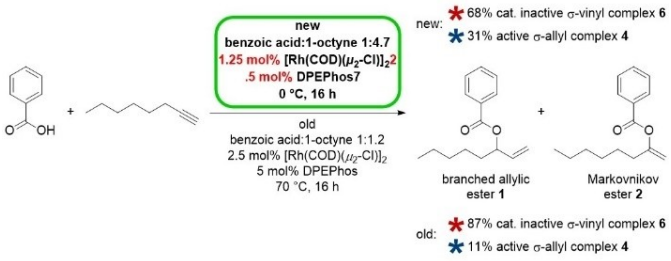

Scheme 4. Optimized rhodium complex catalyzed propargylic C–H activation; the catalyst concentration given is based on the amount of used benzoic acid.

Conclusion

Besides detailed kinetic measurements by using in situ operando NMR spectroscopic reaction monitoring, the studies presented include mechanistic investigations by using NMR and Raman spectroscopy as well as the structural characterization of intermediates of the catalytic cycle with X-ray crystal structure analysis. Especially the interpretation of NMR data by using so-

called *concentration diagrams* provided important information on the parallel formation of the ester products and the generation of the catalytically inactive species **6**. On the basis of these studies, individual elementary steps of the catalytic propargylic C–H activation reaction by using the precatalyst [Rh(DPEPhos)(μ_2-Cl)]$_2$ **7** could be specifically investigated. Thus, although this method is rarely used, its application to complex catalytic reactions is a very valuable tool.

The suspected catalyst deactivation could be confirmed experimentally for the first time by identifying a catalytically inactive rhodium(III) σ-vinyl species **6**, which is formed from a rhodium(III) benzoate complex **10** at low alkyne concentrations. After considering these new insights into the reaction pathway for optimizations of the catalytic protocol, it was possible to more than double the productivity of the catalyst system in initial test reactions. Further studies will focus on the optimized slow addition of benzoic acid for example by syringe pump in combination with in situ IR-spectroscopy to minimize the catalyst deactivation.

Experimental Section

For experimental details, see the Supporting Information.

Crystal-structure analysis: Deposition Numbers 2000244 (**6**), 2000245 (**9**) and 2000243 (**12**) contain the supplementary crystallographic data for this paper. These data are provided free of charge by the joint Cambridge Crystallographic Data Centre and Fachinformationszentrum Karlsruhe Access Structures service www.ccdc.cam.ac.uk/structures.

Acknowledgements

We thank the DFG for the financial support (grant No. HE2890/7-1 and BR1646/10-2). Open Access funding enabled and organized by Projekt DEAL.

Conflict of Interest

The authors declare no conflict of interest.

Keywords: catalyst deactivation · concentration diagrams · C–H activation · kinetics · rhodium catalysis

[1] a) A. Lumbroso, M. L. Cooke, B. Breit, *Angew. Chem. Int. Ed.*, **2013**, *52*, 1890–1932; *Angew. Chem.* **2013**, *125*, 1942–1986; *Angew. Chem. Int. Ed.* **2013**, *52*, 1890–1932; b) J. F. Hartwig, L. M. Stanley, *Acc. Chem. Res.* **2010**, *43*, 1461–1475.

[2] a) B. M. Trost, D. L. van Vranken, *Chem. Rev.* **1996**, *96*, 395–422; b) B. M. Trost, L. M. Crawley, *Chem. Rev.* **2003**, *103*, 2921–2944; c) Z. Lu, S. Ma, *Angew. Chem. Int. Ed.* **2008**, *47*, 258–297; *Angew. Chem.* **2008**, *120*, 264–303.

[3] a) M. S. Chen, M. C. White, *J. Am. Chem. Soc.* **2004**, *126*, 1346–1347; b) G. Liu, S. S. Stahl, *J. Am. Chem. Soc.* **2007**, *129*, 6328–6335; c) G. Yin, Y. Wu, G. Liu, *J. Am. Chem. Soc.* **2010**, *132*, 11978–11987.

[4] a) B. M. Trost, W. Brieden, K. H. Baringhaus, *Angew. Chem. Int. Ed. Engl.* **1992**, *31*, 1335–1336; *Angew. Chem.* **1992**, *104*, 1392–1394; *Angew. Chem. Int. Ed.* **1992**, *31*, 1335–1336; b) Y. Yamamoto, M. Al-Masum, N. Asao, *J. Am. Chem. Soc.* **1994**, *116*, 6019–6020; c) B. M. Trost, V. J. Gerusz, *J. Am. Chem. Soc.* **1995**, *117*, 5156–5157; d) Y. Yamamoto, M. Al-Masum, N. Fujiwara, N. Asao, *Tetrahedron Lett.* **1995**, *36*, 2811–2814; e) B. M. Trost, P.-Y. Michellys, V. J. Gerusz, *Angew. Chem. Int. Ed. Engl.* **1997**, *36*, 1750–1753; f) M. Al-Masum, Y. Yamamoto, *J. Am. Chem. Soc.* **1998**, *120*, 3809–3810; g) I. Kadota, A. Shibuya, Y. S. Gyoung, Y. Yamamoto, *J. Am. Chem. Soc.* **1998**, *120*, 10262–10263; h) N. T. Patil, N. K. Pahadi, Y. Yamamoto, *Synthesis* **2004**, 2186–2190; i) N. T. Patil, F. Nawaz Khan, Y. Yamamoto, *Tetrahedron Lett.* **2004**, *45*, 8497–8499; j) N. T. Patil, N. K. Pahadi, Y. Yamamoto, *Can. J. Chem.* **2005**, *83*, 569–573.

[5] A. Lumbroso, P. Koschker, N. R. Vautravers, B. Breit, *J. Am. Chem. Soc.* **2011**, *133*, 2386–2389.

[6] P. Koschker, M. Kähny, B. Breit, *J. Am. Chem. Soc.* **2015**, *137*, 3131–3137.

[7] A. Lumbroso, N. Abermil, B. Breit, *Chem. Sci.* **2012**, *3*, 789–793.

[8] a) K. Xu, V. Khakyzadeh, T. Bury, B. Breit, *J. Am. Chem. Soc.* **2014**, *136*, 16124–16127; b) T. M. Beck, B. Breit, *Org. Lett.* **2016**, *18*, 124–127; c) A. M. Haydl, L. J. Hilpert, B. Breit, *Chem. Eur. J.* **2016**, *22*, 6547–6551.

[9] a) T. M. Beck, B. Breit, *Eur. J. Org. Chem.* **2016**, 5839–5844; b) C. Li, C. P. Grugel, B. Breit, *Chem. Commun.* **2016**, *7*, 5840–5843; c) Z. Liu, B. Breit, *Angew. Chem. Int. Ed.* **2016**, *55*, 8440–8443; *Angew. Chem.* **2016**, 128, 8580–8583; d) J. Kuang, S. Parveen, B. Breit, *Angew. Chem. Int. Ed.* **2017**, *56*, 8422–8425; *Angew. Chem.* **2017**, *129*, 8542–8545; e) D. Berthold, B. Breit, *Org. Lett.* **2018**, *20*, 3, 598–601; f) J. Zheng, B. Breit, *Angew. Chem. Int. Ed.* **2018**, *58*, 3392–3397; *Angew. Chem.* **2018**, *131*, 3430–3435.

[10] a) U. Gellrich, A. Meissner, A. Steffani, M. Kähny, H. J. Drexler, D. Heller, D. A. Plattner, B. Breit, *J. Am. Chem. Soc.* **2014**, *136*, 1097–1104; b) P. Koschker, B. Breit, *Acc. Chem. Res.* **2016**, *49*, 1524–1536.

[11] R. Shintani, W. L. Duan, S. Park, T. Hayashi, *Chem. Commun.* **2006**, 3646–3647.

[12] C. M. Ting, Y. L. Hsu, R. S. Liu, *Chem. Commun.* **2012**, *48*, 6577–6579.

[13] Test reactions with the precatalyst and the alkyne under the exclusion of benzoic acid have shown that the *dimeric* alkyne is formed instead of the diene. The diene detected during catalysis should therefore result from a complex of the catalytic cycle.

[14] A "resting state" is typically defined as the coordination compound that is present in highest concentration under stationary conditions. It should however be kept in mind that in catalysis that can be described using Michaelis-Menten type kinetics, the pre-equilibrium between catalyst and catalyst-substrate complex can be altered by modification of experimental conditions (such as substrate concentration), which in consequence changes the resting state during catalysis.

[15] a) H. Mauser, *Formale Kinetik-Experimentelle Methoden der Physik und der Chemie*, Bertelsmann Universitätsverlag, **1974**; b) J. Polster, *Talanta* **1984**, *31*, 113–116; c) B. Ursin, H. Kleindienst, *Zeitschrift für Naturforschung* **1986**, *41*, 989–997; d) H. Mauser, G. Gauglitz *Photokinetics: Theoretical Fundamentals and Applications.* Elsevier, **1998**.

[16] Even if the equilibrium between the allyl complexes **4** and **5** is not adjusted, the sum of both complex species does not change and is therefore independent of the status of the equilibrium. For this reason, the *sum* of the allyl complexes was plotted as a function of the percentage of catalytically inactive species **6** in the concentration diagram.

[17] G. Socrates, in *Infrared and Raman Characteristic Group Frequencies: Tables and Charts*, Wiley, **2004**.

[18] Based on the initial part of the concentration-time data (ca. 30–40% conversion) of the reaction monitoring the formation rate of the esters **1** and **2**, the benzoate complex **12** and the σ-vinyl compound **6** have been determined. For this purpose, the sum of two exponential functions was chosen as a differentiable substitute function, whereby this corresponds to the respective initial rate at time $t = 0$ (calculation example in Figure S30).

[19] A. Mannu, M. Ferro, S. Möller, D. Heller, *J. Chem. Res.* **2018**, *42*, 402–404.

[20] The doublet as coupling pattern in the ^{31}P NMR spectrum shows that the molecule is probably symmetrical and therefore does not correspond to the originally postulated asymmetrical compound [RhCl-(DPEPhos)(1-octyne)]. In addition, the resulting species cannot be converted with benzene to an arene complex, so it can be assumed that it is not cationic. (C. Fischer, R. Thede, H.-J. Drexler, A. König, W. Baumann, D. Heller, *Chem. Eur. J.* **2012**, *18*, 11920–11928). By adding 1-octyne to the pentacoordinated complex [RhCl(DPEPhos)(NBD)], (A. Meißner, A. König, H.-J. Drexler, R. Thede, C. Fischer, W. Baumann, D. Heller, *Chem. Eur. J.* **2014**, *20*, 14721–14728) the species sought can be detected spectroscopically by ^{31}P NMR. It can be concluded that the signal (22.4 ppm; d, $J_{RhP} = 117$ ppm) can be assigned to the *pentacoordinated* species [RhCl(DPEPhos)(1-octyne)$_2$].

[21] S. Möller, H.-J. Drexler, D. Heller, *Acta Crystallogr.* **2019**, *C75*, 1434–1438.
[22] In order to test the reversibility of the formation of this new compound, the reaction mixture of precatalyst and 1-octyne was evacuated. If the reaction to the new alkyne complex is irreversible, no signals from the precatalyst should be detectable after removal of the alkyne by vacuum. However, it can be observed that after reducing the alkyne concentration in solution, more than half of the alkyne complex has been transformed into other phosphorus-containing rhodium complexes, including the precatalyst.
[23] The signals of the dimeric alkyne were found only under exclusion of benzoic acid, but not in the catalytic reaction.
[24] The remaining 1-octyne due to the stoichiometry of the reaction could be separated from the products and reused after the catalytic reaction is completed.

Manuscript received: June 21, 2021
Accepted manuscript online: July 14, 2021
Version of record online: August 1, 2021

